Footstep Planning for Slippery and Slanted Terrain Using Human-Inspired Models

Martim Brandão, *Member, IEEE*, Kenji Hashimoto, *Member, IEEE*, José Santos-Victor, *Senior Member, IEEE*, and Atsuo Takanishi, *Member, IEEE*

***Abstract*—Energy efficiency and robustness of locomotion to different terrain conditions are important problems for humanoid robots deployed in the real world. In this paper, we propose a footstep-planning algorithm for humanoids that is applicable to flat, slanted, and slippery terrain, which uses simple principles and representations gathered from human gait literature. The planner optimizes a center-of-mass (COM) mechanical work model subject to motion feasibility and ground friction constraints using a hybrid A* search and optimization approach. Footstep placements and orientations are discrete states searched with an A* algorithm, while other relevant parameters are computed through continuous optimization on state transitions. These parameters are also inspired by human gait literature and include footstep timing (double-support and swing time) and parameterized COM motion using knee flexion angle keypoints. The planner relies on work, the required coefficient of friction (RCOF), and feasibility models that we estimate in a physics simulation. We show through simulation experiments that the proposed planner leads to both low electrical energy consumption and human-like motion on a variety of scenarios. Using the planner, the robot automatically opts between avoiding or (slowly) traversing slippery patches depending on their size and friction, and it chooses energy-optimal stairs and climbing angles in slopes. The obtained motion is also consistent with observations found in human gait literature, such as human-like changes in RCOF, step length and double-support time on slippery terrain, and human-like curved walking on steep slopes. Finally, we compare COM work minimization with other choices of the objective function.**

***Index Terms*—Biologically inspired robots, footstep planning, human gait, humanoid robots, motion planning, path planning.**

Manuscript received February 06, 2016; accepted May 17, 2016. Date of publication July 13, 2016; date of current version August 18, 2016. This paper was recommended for publication by Editor A. Kheddar and Guest Editors K. Mombaur and D. Kulic upon evaluation of the reviewers' comments. This work was supported by Japan Society for the Promotion of Science Grants-in-Aid for Scientific Research under Grant 15J06497 and Grant 25220005, and by the ImPACT TRC Program of Council for Science, Technology and Innovation, Cabinet Office, Government of Japan. This work was also supported by Project FCT [UID/EEA/50009/2013] and Project EU Poeticon++.

M. Brandão is with the Graduate School of Advanced Science and Engineering, Waseda University, Tokyo 162-0044, Japan (e-mail: mbrandao@fuji.waseda.jp).

K. Hashimoto is with the Waseda Institute for Advanced Study and the Humanoid Robotics Institute, Waseda University, Tokyo 162-0044, Japan (e-mail: hashimoto@aoni.waseda.jp).

J. Santos-Victor is with the Institute for Systems and Robotics, Instituto Superior Técnico, Universidade de Lisboa, 1049-001 Lisboa, Portugal (e-mail: jasv@isr.tecnico.ulisboa.pt).

A. Takanishi is with the Modern Mechanical Engineering and the Humanoid Robotics Institute, Waseda University, Tokyo 169-8555, Japan (e-mail: takanisi@waseda.jp).

Color versions of one or more of the figures in this paper are available online at http://ieeexplore.ieee.org.

Digital Object Identifier 10.1109/TRO.2016.2581219

I. Introduction

HUMANOID robot locomotion planning is an important problem with applications in disaster response and service. Footstep-planning algorithms are a computationally attractive solution to the locomotion problem, since they reduce the search space from whole-body motion to footstep positions and orientations. Current footstep planners excel at obstacle avoidance but do not consider important factors such as ground friction and energy consumption. These factors are especially important in outdoor environments where the robot will depend on batteries and surface conditions might be challenging: slippery, inclined, etc. While it still is not clear how footstep planners should be formulated in order to consider many such factors, our claim in this paper is that using principles and representations in human gait literature can lead to naturally improved footstep planning. Namely, in this paper we integrate human-inspired center-of-mass (COM) work and required coefficient of friction (RCOF) models as functions of footstep displacement, timing, and parameterized COM motion into a new hybrid search-optimization planner, obtaining friction-aware low-electrical-power footstep plans.

The contributions of this paper are the following:

1) We give an overview of anticipatory human gait literature and identify principles and representations useful to humanoid locomotion in a variety of scenarios.
2) We propose a footstep-planning algorithm based on 1, which plans both footstep positions, orientations, timing, and parameterized COM motion.
3) We show that the proposed method applied to the WABIAN-2 robot leads to walking motion observations consistent with those seen in human gait literature.
4) We show that paths obtained with the proposed planner also lead to low electrical energy consumption.

This paper is related to two previous publications, [1] and [2]. Compared with these, we:

1) further extend the models and planner to account for locomotion on slopes;
2) give an overview of anticipatory human gait literature relevant to footstep planning, explaining the motivations behind our choice of optimization objectives, constraints, and variables;
3) claim human likeness of the motion obtained with our planner by comparing it with observations in human gait.

II. Related Work

A. Humanoid Footstep Planning

In humanoid walking, as in human gait literature, it is common to distinguish two levels of locomotion control: planning

and feedback control. In this paper, we focus on the (footstep) planning problem for humanoids. This problem is closely related to the study of anticipatory human gait adaptations. For example, representations of walking used in human gait literature to describe anticipatory gait control are closely related to those used in high-level motion-planning algorithms in robotics, such as footstep planning, contact planning, and other task-space planning approaches. Both typically deal with observations in terms of a high-level representation of walking such as modality, foot position, orientation, timing, limb stiffness, or COM height.

For humanoids, the footstep- and contact-planning problems have been tackled with search [3]–[7], sampling [8], and optimization [9], [10] algorithms. Search-based planners such as A* [3]–[5] and its variants [6], [7] have been used successfully to plan obstacle-free paths in both static and dynamic [5] scenarios. Recently, purely optimization-based planners have also been proposed [10], which eliminate the suboptimal discretization problem inherent to search-based planners. Sampling-based planners [8], allowing for multiple contacts (e.g., hands, knees), are useful for very complex environments, although at a high computational cost, which can be slightly ameliorated with a good selection and adaptation of motion primitives [11]. While the aforementioned planners focus on finding collision-free paths, the methods in this paper go one step further by considering energy, collision, and friction.

One important step in footstep planners is to estimate whether or not a given stance or step is feasible. Some authors opt to approximate feasibility by rough reachability of the feet [7], full inverse kinematics feasibility [8], or smart collision checking [12]. In this paper, we use both rough reachability intervals to discard obvious unfeasible poses, as in [7], but also learn a model of feasibility from physics simulation, in which feasibility is both static and dynamic.

Research closely related to this paper includes [3], in which terrain and energy-related cost functions are used in A* search to compute optimal cost plans. They sum a set of empirical human biomechanics-inspired models of energy cost that are polynomial functions of step length, width, and rotation. In addition, Kim, Pollard, and Atkeson [4] use a similar approach, with quadratic cost functions on sequences of footstep positions. On the other hand, in this paper we also consider timing variables and surface friction. We do not assume polynomial relationships and instead use an off-the-shelf machine-learning algorithm to learn the relationship between variables from data. And, finally, we make claims concerning energy consumption and human-like motion.

In this paper, we prevent slippage of the robot by planning, which complements other feedback control approaches to friction-constrained biped walking [13]–[15]. While feedback control can help to reduce tangential-to-normal force ratios locally, it may not be sufficient in very-low-friction surfaces. For example, a robot with rubber soles would be subjected to less than 0.15 kinetic friction when walking on ice. Slipping can be reduced in such low-friction floors without changing gait, but it is not eliminated [13]. Feedback control approaches usually consist of friction cone constraints in inverse dynamics [16] or operational space control framework [15]. Design parameters in the preview controller [17] can also be slightly tuned to reduce the RCOF for a fixed gait, and feedback ZMP controllers can be manually adapted to account for friction [13]. Efforts have also been put into reactive reflex controllers that, without changing gait parameters, try to reduce slipping after it is detected (e.g., by waist or foot acceleration reflexes [14]). In this paper, we take the complementary high-level approach by optimizing energy and eliminating slippage as much as possible by changes in gait. Such an approach solves the known problem of reactive controllers to not be able to avoid slipping on fast gait [14] and, at the same time, leverages human gait literature findings supporting energy and stability optimization at the footstep level, which is not just reactively but also anticipatorily controlled.

B. Anticipatory Gait Control in Humans: Human Gait Is Planned

The claim that humans also plan gait, and footsteps in particular, is supported by evidence in both children and adults. For example, children walkers (average age 14 months) switch walking modality from bipedal to quadrupedal on a waterbed after visual inspection of its waviness or haptic exploration [18]. Children also use haptic exploration on slopes to decide whether to walk, crawl, slide down in sitting or backing positions, or to not traverse them at all [19].

Across numerous studies of adult human walking, there is also the observation of a "cautious gait" style used in uncertain environments [20]–[22] or after sensory loss [23], [24]. For example, the authors of [20]–[22] observed a specific cautious gait mode when there is awareness of a slippery surface, which is then adapted to the specific slipperiness condition found. On slippery surfaces, typically, walking speed is decreased, the COM is centered over the supporting limb, and limb stiffness is increased [20]–[22]. Even when there is no knowledge of the degree of slipperiness, stride length [20], [21], [25], foot contact angle [22], [25]–[27], and vertical heel contact velocity [26] decrease, while knee flexion increases [22], [27]. According to [22], these surface-approach changes are learned through prior slip experience and are applied to different conditions when surface properties are unknown. Further knowledge of the coefficient of friction changes muscle activation and how the foot interacts with the floor. On slippery terrain, both these gait and muscle activation patterns become characteristically different since the first step on the surface, which indicates an anticipation strategy and not reactive adaptation of normal gait. A cautious gait is also used in other uncertain circumstances, such as when vision is blurred by light-scattering lenses [23]. Another interesting observation is that human walking trajectories on steep slopes such as mountains or hills are not straight least-distance paths but more energy-efficient curved paths uphill [28], [29]. Interestingly, Proffitt, Bhalla, Gossweiler, and Midgett [30] showed that visual perception of slant changes from viewpoint (downhill looks steeper and is also more difficult), which suggests that climbing gradients could be a result of the perception of slant.

All these examples show how humans adapt high-level gait parameters such as modality, footstep position, and timing or COM trajectories by some sort of motion planning based on visual or haptic perception of the environment.

Part of these observations have been obtained in robotics and animation literature by optimization algorithms; for example, lower step lengths [1], [31] and lower COM [31] on slippery terrain. Wang, Fleet, and Hertzmann [31] achieved this by a low-level joint controller, while Brandão, Hashimoto, Santos-Victor, and Takanishi [1] used a footstep-planning algorithm. The latter planner-based approach is more easily adaptable to complex terrain with obstacles and slopes. In this paper, we extend its methods further, obtaining several human-like walking behavior observations both in slippery terrain and slopes.

C. Human Gait as Optimization in High-Level Representation: Variables and Objectives

The optimal gait of humans, according to [28], is related to fitness of the species and is a function of several factors such as speed, acceleration, endurance, energy, and stability. Human gait studies have shown that these attributes can be modeled by simple principles and using equally simple high-level representations of gait. For example, step length and cadence have been shown to have a linear relationship [32]. In addition, simple empirical equations of step length and step rate proposed by Zarrugh, Todd, and Ralston [33] lead to contours of energy consumption per meter, which match subject data from different studies. In particular, the metabolic "cost of transport" (energy per unit distance) is a frequent optimization objective studied in human gait literature. Humans have been shown to choose an average step length and frequency that minimizes average energy cost per distance [33]–[36]. Minimization of vertical cost of transport, mainly by regulation of COM height, also explains locomotion patterns on steep slopes as shown by Minetti [29]. Studies usually model energy as oxygen consumption [33], joint or muscular work [37], and body or COM work [38]. Energy recovery [39] of the COM also is another considered objective related to COM work.

The previously stated measurements have been shown to vary systematically with high-level gait parameterizations such as step length [19]–[21], [25], [40], step width [25], speed [20], [27], [40], COM height [20], knee flexion at heel strike [22], foot angle and velocity at heel strike [21], [25], [26], [41], double-support and swing times [27], [32], [41], and limb stiffness [20]. The same variables have also been shown to be used, whether directly or indirectly, to regulate the RCOF: the ratio of shear to normal ground reaction force (i.e., tangential to normal force) [20]–[22]. The RCOF constraint should be kept below the ground's coefficient of friction to avoid slips and consequent falls, but it is planned and not just controlled reactively [20].

Travel time, acceleration, and orientation error also are other functions that can be optimized to predict COM trajectories in flat goal-directed paths indoors [42].

III. Our Humanoid Footstep-Planning Model

From the anticipatory gait control studies mentioned in the previous section, we selected simple optimization objectives and variables such that: 1) they are easily applicable to current humanoid-locomotion-planning algorithms, namely footstep planning; and 2) they predict walking behavior observations in different human gait literature for a variety of scenarios. In particular, we focus on observations on slippery environments, and on flat and slanted terrain.

Based on these criteria, we selected the following optimization variables: *Step length, width, and height:* As discussed in Section II-C, both energy and RCOF have been shown to vary systematically with these variables. In addition, their application to robot footstep planning is straightforward since these are simple distances between feet. *Double-support time and leg swing time:* As discussed, these vary systematically in adaptations to slippery terrain. Inclusion in (extended) footstep planning adds flexibility to the planner to lower gait accelerations and may thus allow the robot to navigate more slippery terrain, as initially proposed in [1]. *Knee flexion angles:* These also vary systematically in adaptations to slippery terrain [22]. Furthermore, they are related to COM height, which explains adaptations in steep slopes and slippery terrain. For robot locomotion, planning COM trajectories is also crucial for stability and feasibility considerations. In this paper, we parameterize the COM height trajectory through inflexion points of a knee angle trajectory spline.

We define and learn optimization objectives and constraints, in simulation as functions of the previously stated variables. The models we borrow from human gait literature are as follows. *COM work as optimization objective:* As discussed in Section II-C, energy optimization, and in particular COM work, explains walking patterns in both flat and sloped terrain [29], [35]. The advantage of this model for robotics when compared with, for example, electrical energy or torque minimization is basically its simplicity. Since only COM velocity and force profiles are required to estimate COM work, it applies to both complex robot models and simple single-mass robot models. There is also the motivation of passive dynamic walkers [43], which optimize COM work by construction. *RCOF as a constraint:* As discussed, RCOF has been shown to vary on slippery terrain. While it is not clear whether RCOF should be used as a hard or soft constraint in order to explain human data, in this paper we opt for a hard constraint. We assume Coulomb friction and set RCOF$< \mu$ as a constraint in the problem, which is advantageous from a conservative perspective, to theoretically avoid slipping and thus not have to rely heavily on reactive slippage control.

As we will show in Section VI, our footstep-planning model leads to the following human-gait-predicted behavior.

1) Energy contours are hyperbolic in the step length rate [33], [35].
2) RCOF is reduced on slippery terrain [21].
3) Step length is reduced on slippery terrain [20], [21], [25].
4) Double-support time is increased on slippery terrain [27].
5) There is an optimal climbing angle for steep slopes [28], [29]. In other words, long steep trajectories will be curved.

A. Problem Statement

We consider the problem of finding a sequence of N footsteps $f_j = (x_j, y_j, z_j, \theta_j) \in \mathbb{R}^4,\ j = 1, \ldots, N$, such that energy is minimized and with feasibility and no-slippage as constraints. The plan starts at a fixed initial stance $s_1 = (f_1, f_2)$ and finishes at a fixed goal stance $s_{N-1} = (f_{N-1}, f_N)$. N is unknown; (x_j, y_j, z_j) and θ_j are position and yaw orientation of a foot in

a global coordinate frame. For convenience, f_j is a left foot if j is odd, and right if j is even. The energetic cost E_{COM} of transitioning from a stance s_{j-1} to s_j depends on both the stances and some extra parameters $p_j \in \mathbb{R}^P$. p represents state transition parameters that might provide different ways for s_j to be reached from s_{j-1}, such as step timing and COM motion. In this paper, we use $p_j = (\Delta t_{\text{ds}}, \Delta t_{\text{sw}}, \phi_0, \phi_{\text{st}}, \phi_{\text{sw}}) \in \mathbb{R}^5$, which are double-support time (i.e., time spent on s_{j-1}), swing time (i.e., time spent with the swing leg in the air), and minimum knee flexion, maximum stance knee flexion, and maximum swing knee flexion angles. Throughout the paper, we will also refer to a state (i.e., stance) transition as a "step."

The general problem we are trying to solve in this paper is

$$\begin{aligned}
&\text{minimize} \\
&N, f_3..f_{N-2}, p_2..p_{N-1} \quad \sum_{j=2\ldots N-1} E_{\text{COM}}(f_{j-1}, f_j, f_{j+1}, p_j) \\
&\text{subject to} \\
&\text{RCOF}(f_{j-1}, f_j, f_{j+1}, p_j) < \min(\mu_{j-1}, \mu_j, \mu_{j+1}) \\
&\Psi(f_{j-1}, f_j, f_{j+1}, p_j) < 0 \\
&a < p_j < b
\end{aligned} \tag{1}$$

where the function Ψ implements feasibility constraints on the stances and steps due to kinematic, dynamic, or controller limitations. We assume that a coefficient of friction μ_j is known for each f_j and a Coulomb friction model so that RCOF is a tangential-to-normal force ratio. Bound constraints on the step parameters are implemented with vectors a and b.

IV. Obtaining Energy, Required Coefficient of Friction, and Feasibility Models

A. Definitions

We compute total COM mechanical work as

$$E_{\text{COM}} = \int_{t_0}^{t_1} |\mathbf{v}.\mathbf{F}| dt \tag{2}$$

where $\mathbf{v}$ and $\mathbf{F}$ are the velocity and total force vectors at the COM, respectively, and t_0 and t_1 are the beginning and ending time of a step (i.e., $t_1 - t_0 = \Delta t_{\text{ds}} + \Delta t_{\text{sw}}$).

RCOF [21] is defined as the maximum ratio of tangential-to-normal force applied at the feet during a given step as

$$\text{RCOF} = \max_{t \in [t_0; t_1]} \left| \frac{F_{\text{T}}(t)}{F_{\text{N}}(t)} \right| \tag{3}$$

where F_{T} is the tangential force and F_{N} is normal force at the feet. In this paper, we assume a Coulomb friction model. Therefore, note that if RCOF is lower than the actual coefficient of friction between feet and floor, slippage is theoretically prevented during that step.

Finally, we define the feasibility model as $\Psi \in \{-1, 1\}$ and use value 1 for unfeasible points and -1 for feasible. To discard obvious unfeasible stances, we first use a footstep parameterization as in [7] to obtain a heuristic approximation of footstep reachability: in a stance s_j, reachability is approximated by a set of intervals for the variables $(\Delta x_{j+1}, \Delta y_{j+1}, \Delta z_{j+1}, \Delta \theta_{j+1})$, which are distances from the first footstep to the second, i.e., $\Delta x_{j+1} = x_{j+1} - x_j$, etc. Stances outside these intervals are considered to be unfeasible with $\Psi = 1$. Steps are also considered to be unfeasible if COM motion respecting the reference ZMP trajectory cannot be found using our walking pattern generator [44], joint limits are reached, or the robot falls during physics simulation.

B. Implementation

During a training stage, we run physics simulations exploring the space of steps $(f_{j-1}, f_j, f_{j+1}, p_j)$ and collecting measurements of E_{COM}, RCOF, and Ψ. Each simulation consists of a symmetric and periodic gait of steps with constant step length, width, height, and p. The patterns also start and finish with zero COM velocity and are stabilized with the pattern generator described in [44]. We train an infinite mixture of linear experts (IMLE) [45] for each model as a function $\hat{f} : \mathbb{R}^{3+P} \rightarrow \mathbb{R}$, where inputs are the variables mentioned previously (i.e., step length, width, height, and p) and outputs are the measurements E_{COM}, RCOF, and Ψ. Since the simulations consist of symmetric periodic gait, step lengths (usually defined as the distance between two consecutive feet at heel strike [22]) are the same as stance lengths, and likewise for width and height.

We chose to use IMLE for function approximation due to its high query speed and low number of experts, while still allowing for online learning if necessary. Error performance is comparable with that of Gaussian processes [45]. Models were trained by uniform sampling of the input space and using the necessary number of experts to obtain a standardized mean squared error lower than 0.1.

In the case of the feasibility function, we still fit a continuous mixture model even though training points are discrete $\Psi \in \{-1, 1\}$, leading to interpolation regions between -1 and 1. While planning, we enforce a slightly conservative feasibility constraint of $\Psi < 0$ to avoid uncertain regions far from feasibility ($\Psi = -1$).

V. Solving the Planning Problem

A. Discretized Search of Footsteps, Continuous Optimization of Step Parameters

In this paper, we solve (1) by a hybrid discrete search and continuous optimization-based planner. We first constrain the footstep (position) space to a point cloud of traversable points $(x, y, z) \in \mathbb{R}^3$ and a discrete set of orientations in the global coordinate frame $\theta \in \{0^\circ, \frac{360}{D}^\circ, \ldots, \frac{360(D-1)}{D}^\circ\}$, where D is the number of uniform footstep directions. Then we compute the optimal-cost path from the initial to goal stance on this space using anytime repairing A* (ARA*) [46]. ARA* requires a state transition cost function $c(s_{j-1}, s_j)$ and a heuristic cost-to-go function $h(s_j)$. It will find the optimal path to the goal given enough computation time and an admissible h. If interrupted at any time, then the algorithm still returns a suboptimal path with provable bounds. See [46] for further details.

In our case, the state transition cost $c(s_{j-1}, s_j)$ is the minimum-energy transition between the two consecutive

stances $s_{j-1} = (f_{j-1}, f_j)$ and $s_j = (f_j, f_{j+1})$, given by

$$\begin{aligned} c(s_{j-1}, s_j) = \; & \min_{p_j} \; E_{\text{COM}}(f_{j-1}, f_j, f_{j+1}, p_j) \\ & \text{subject to} \\ & \text{RCOF}(f_{j-1}, f_j, f_{j+1}, p_j) < \min(\mu_{j-1}, \mu_j, \mu_{j+1}) \\ & \Psi(f_{j-1}, f_j, f_{j+1}, p_j) < 0 \\ & a < p_j < b. \end{aligned} \tag{4}$$

Hence, even though states in A* search are discretized stances, step parameters are computed from continuous optimization on the state transitions.

Regarding the heuristic $h(s_j)$, we set it equal to a lower bound on the cost from s_j to the goal, which assumes no obstacles, optimal cost of transport, and infinite friction. In this way, $h(s_j)$ never overestimates the true cost to the goal (i.e., is admissible), as required for A* optimality. We compute the bound as the minimum horizontal cost of transport times distance as

$$\begin{aligned} h(s_j) = \; & d_{xy}(s_j, s_{N-1}). \min_{f_k, f_{k+1}, p_k} \frac{E_{\text{COM}}(f_{k-1}, f_k, f_{k+1}, p_k)}{||(x,y)_{k+1} - (x,y)_{k-1}||} \\ & \text{subject to} \\ & \Psi(f_{k-1}, f_k, f_{k+1}, p_k) < 0 \\ & a < p_k < b \end{aligned} \tag{5}$$

where $d_{\text{xy}}(s_j, s_{N-1})$ is the Euclidean distance on the horizontal plane from stance s_j to stance s_{N-1} (i.e., the distance between left feet and the right feet summed). True costs to goal will actually be higher than (5), since optimal step parameters might not be feasible for the whole distance and more costly paths might be necessary due to kinematics constraints, obstacles, friction, or slope.

In practice, we precompute and store on a hash table the results of (4) for a large number of footstep displacements and coefficients of friction. Similarly, we only need to solve the optimization problem in (5) once. Planning a path from an initial stance s_1 to a goal stance s_{N-1} then consists of a straightforward ARA* (or A*) search in which each time a state transition is considered, we access a hash table to obtain the state transition cost (4) and then compute the heuristic cost-to-go from the distance to goal and the precomputed cost-of-transport using (5).

B. Implementation

We implement point cloud discretization with Point Cloud Library [47] using 5-cm grid-filtered point clouds. The search for successors of a stance is done by a range search of points around the fixed foot. In addition, the directions of footsteps were discretized uniformly with $D = 24$.

We use the official implementation of ARA* [46] in the Search-Based Planning Library [48]. Optimization problems (4) and (5) are first solved with the global optimization algorithm DIRECT [49], which is then refined using the sequential quadratic programming algorithm SLSQP [50]. Both optimization algorithms are implemented in the NLOpt library [51]. The functions E_{COM}, RCOF, and Ψ are each implemented as an IMLE, as described in Section IV-B.

During ARA* search, we use precomputed versions of (4) for speed. After the final solution is obtained, we further refine the step parameters p by solving (4) using SLSQP, warm-started by the values stored on the hash table.

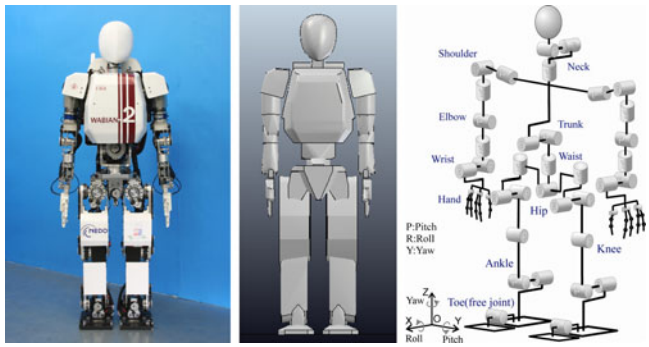

Fig. 1. WABIAN-2 humanoid robot used in our simulation experiments. From left to right: real robot, simulated, and DOF.

VI. Results

A. Platform and Setup

All experiments described in this paper were conducted on a simulated model of humanoid robot WABIAN-2, shown in Fig. 1. WABIAN-2 is a human-sized humanoid robot, 1.5-m tall, weighting 64 kg, and with 41 DOFs. Joints are driven by DC motors with high gear reduction ratios of around 200.

We used an open dynamics engine (ODE) for physics simulation on the V-REP robot simulator [53], at a 4-ms control cycle (ODE computation time step 1 ms, global ERP 0.8, all other parameters set to their default values). The robot's joints are position controlled using the same gains as the real robot (proportional gain between 0.7 and 0.8). We used the walking pattern generator described in [44], which stabilizes the walking motion based on the robot's full dynamical model and works for varying COM height motion. ZMP reference trajectories were placed at the center of the stance foot during the swing phase and cubic-spline-interpolated to the other foot during the double-support phase. Full trajectories of the knees were obtained by cubic spline interpolation between a minimum flexion angle at impact ϕ_0 and maximum flexion angle at stance ϕ_{st} and swing ϕ_{sw}, as shown in Fig. 2.

The limits of stance reachability were set according to the kinematic chain of WABIAN-2 by manual inspection as follows:

1) $\Delta x \in [0; 0.38]$ m, where x points forward;
2) $\Delta y \in [0.17; 0.30]$ m, where y points to the left (symmetric interval if f_{j+1} is a right foot);
3) $\Delta z \in [-0.15; 0.15]$ m, where z points upward;
4) $\Delta\theta \in [0; 30]$ °, where θ runs counterclockwise (symmetric interval if f_{j+1} is a right foot).

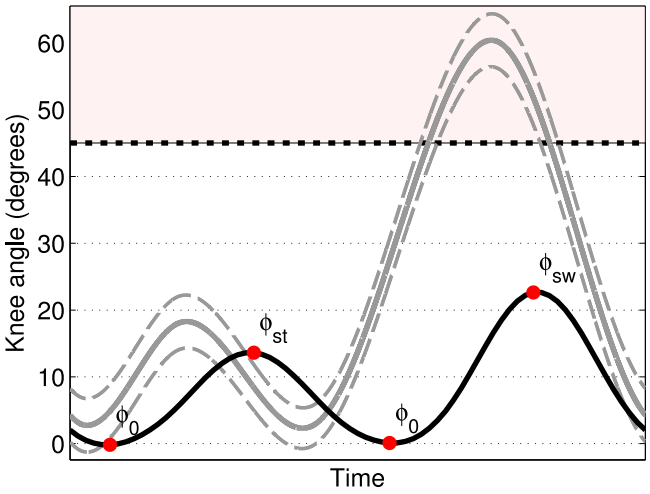

Fig. 2. Knee trajectories used for the robot are interpolated with a cubic spline between a minimum flexion angle ϕ_0 at impact and maximum angles at stance ϕ_{st} and swing ϕ_{sw}. Average and standard deviation of human data is plotted in gray based on [52]. The robot's curve can be made close to that of humans by adjusting double-support time (moving ϕ_0 to the left in this example) and stance angle (ϕ_{st} up); however, ϕ_{sw} cannot exactly match human data ($\phi \leq 45°$, pink region is unfeasible).

The state transition (i.e., step) parameter vector was defined as $p = (\Delta t_{\text{ds}}, \Delta t_{\text{sw}}, \phi_0, \phi_{\text{st}}, \phi_{\text{sw}}) \in \mathbb{R}^5$ and was sampled within the intervals as follows:

1) $\Delta t_{\text{ds}} \in [0.09; 1.8]$; $\Delta t_{\text{sw}} \in [0.9; 1.8]$ s;
2) $\phi_0 \in [1; 21]$ °;
3) $\phi_{\text{st}} \in [5; 45]$; $\phi_{\text{sw}} \in [5; 45]$°.

Due to the high dimensionality of the models, we had to obtain thousands of training points from simulations. To reduce the training time, we trained two separate versions of each model: one for level and one for inclined terrain. We used all dimensions except Δz on the level terrain version and an approximate model on inclined terrain. In the latter, knee trajectories have a narrow feasibility space (collisions, complex motion); therefore, we constrained them to obtain a fixed foot-COM height trajectory. With this approximation, models were learned in around two days of simulation. In total, we generated around 12 600 different walking patterns. Each pattern is a sequence of six symmetric steps of constant step length, width, height, and p. From these simulations, we gathered measurements of E_{COM}, RCOF, and Ψ.

As explained in Section V, we then fitted an IMLE model to the measurements, solved (4) for a large number of footstep displacement and μ values, and stored the results on a hash table. In our experiments, this hash table had 18 491 entries. To solve (4) this many times took approximately 2 h. When planning, we simply query the table to obtain state transition costs and step parameters p from the transitions' footstep displacement and μ values. Query time is at the microsecond level.

B. Models of Energy and Required Coefficient of Friction

Fig. 3 shows the E_{COM} model as a function of step length and height, for two different slope friction values ($\mu = 0.2$ and 0.4). The energy at each steplength–stepheight combination also depends on the other parameters p and, therefore, the minimum

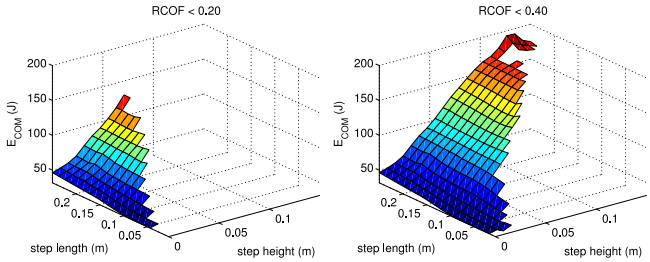

Fig. 3. Minimum E_{COM} on slopes, as a function of step length and step height. Measured in physics simulation.

E_{COM} across p is shown at each point. The gradient of the energy is mainly dominated by the step height value, indicating high energy cost for slanted terrain. The maximum feasible slope angle for each friction value can be seen by the absence of colored energy values and is approximately $18°$ for RCOF < 0.2 and $45°$ for RCOF < 0.4. The high energy cost of slanted terrain actually leads to a preference for shallow walking slopes, as we will show in Sections VI-C and VI-D. Fig. 4 shows the contours of E_{COM} for level walking. The figure shows that most of the energy is spent in double support: the shorter the Δt_{ds}, the lower the energy. Leg swing time mostly does not influence COM energy, which reflects the fact that the alignment of velocity and force are low when compared with double support (motion on the sagittal plane is close to an inverted pendulum).

We show the RCOF model in Fig. 5. RCOF is mainly dependent on the time spent in double support (contours are vertical in the right-most Δt_{ds}, Δt_{sw} plot). The higher the Δt_{ds}, the lower the RCOF. In addition, the lower the step length, the lower the RCOF. Our interpretation is that both increasing Δt_{ds} and decreasing step length lead to lower COM accelerations during double support and thus a more static gait. For this reason, tangential forces are lower and so is RCOF. These observations match human data, as we will discuss in Section VI-D.

C. E_{COM}-Optimal Planning: Resulting Paths and Energetic Advantages

In this section, we analyze the walking paths generated by the described E_{COM}-optimal planner in practice, as well as the paths' expected electrical energy consumption. Our motivation for estimating electrical energy consumption was not only due to its practical value in robotics, but also because mechanical work in humans is related to metabolic energy (i.e., oxygen consumption) [29], [36].

Since the real WABIAN-2's joints are driven by DC motors [54], we compute electrical energy as

$$E_{\text{ele}} = \sum_i \left(\int_{t_0}^{t_1} |\tau_i \omega_i| dt + \int_{t_0}^{t_1} R_i I_i^2 dt \right) \tag{6}$$

where i is an index of the motor, τ is the motor torque, and ω is the angular velocity. I refers to current, which in simulation is computed as $\tau/(r.K_\tau)$, where r is the motor's gear reduction ratio and K_τ is the torque constant, taken from the motors' data sheets. RI^2 are the power losses due to motor armature resistance and we ignore mechanical losses such as joint friction.

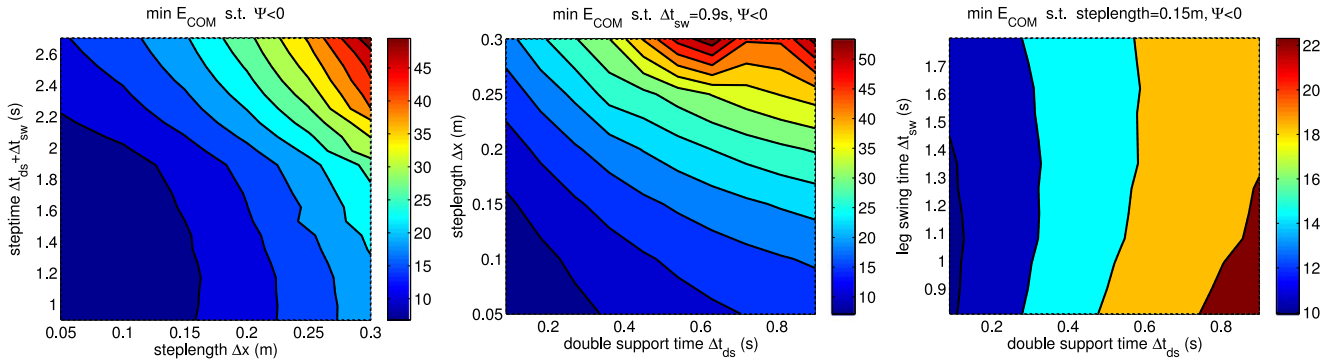

Fig. 4. Minimum E_{COM} measured in physics simulation, on flat terrain.

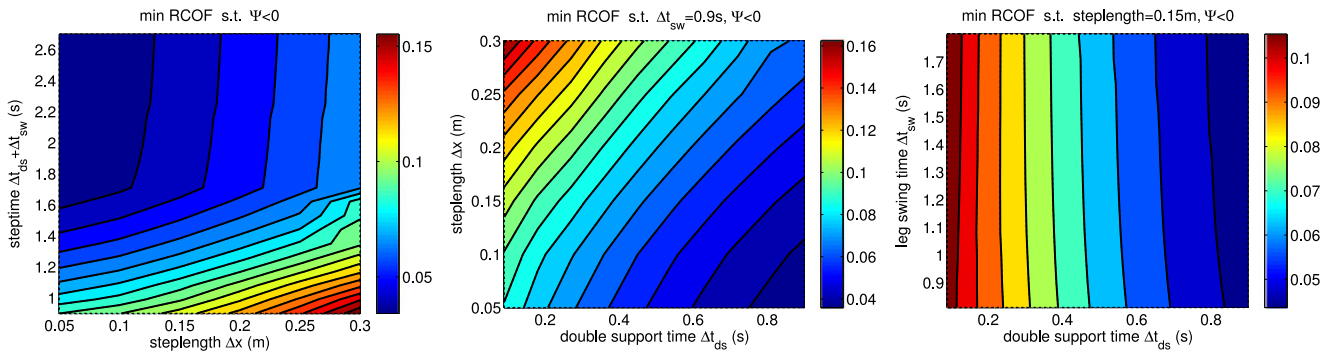

Fig. 5. RCOF, or the maximum ratio of tangential-to-normal force over a step, measured in physics simulation on flat terrain. It indicates the minimum ground coefficient of friction μ, where the robot can walk without slipping.

We compare the resulting electrical energy consumption obtained by our planner with a set of baselines: 1) minimum-travel-time planner; 2) minimum-sum-of-torques planner; and 3) directly optimizing electrical energy consumption E_{ele}, as defined in (6). The results for the baselines were obtained using exactly the same planner equations (4) and (5) and implementation, the only difference being that we replaced E_{COM} with $(\Delta t_{\text{ds}} + \Delta t_{\text{sw}})$, $\int \sum_i \tau_i^2 dt$, and E_{ele}, respectively.

We conducted the experiments in three different scenarios, which we will now describe and analyze. Energy consumption results are reported in Table I.

The first scenario (see Fig. 6) was as follows. The robot stands on the ground with friction $\mu_{\text{ground}} = 1.0$ and has to walk to a target that is straight ahead, 3 m away. Between the start and finish points, there is an "ice patch" of very low friction μ_{ice}. We conducted several planning experiments with different $\mu_{\text{ice}} \in \{0.12, 0.06\}$ and different widths of the ice patch ($\{0.5, 1\}$ m). Fig. 6 shows that, when using our planner, the robot walked through the ice for $\mu_{\text{ice}} = 0.12$ (specifically, it walked 5% slower than the optimal speed with increased double support), but walked around the ice if $\mu_{\text{ice}} = 0.06$. When we doubled the ice patch width but kept the low friction $\mu_{\text{ice}} = 0.06$, and the planner found it more optimal to go through the ice approximately twice as slow (with increased double support) than around a great distance. In terms of expected electrical energy (see Table I), the paths generated by our planner spent 2110, 2427, and 3031 J, respectively. We also conducted experiments constraining the planner to take the alternative, suboptimal choice of avoiding the ice patch when it is optimal to cross it and vice versa. Such suboptimal choices would lead to 14%, 19%, and 10% more electrical energy, respectively. Thus, an increase in COM work (suboptimal plan) leads to an increase in electrical energy consumption. The electrical energy obtained by our optimal planner was relatively close to the real minimum of E_{ele}. Optimizing electrical energy directly lead to 25%, 12%, and 18% less consumption than optimizing COM work. On the other hand, optimizing travel time (common objective function of footstep planners) would lead to drastic energy spending, increasing by 26%, 51%, and 92%. Optimizing joint torques decreased energy spending slightly, by 11%, 3%, and 13%.

The second scenario (see Fig. 7) was as follows. There are two stairs at equal distance to the robot ($x = 1$ m away, $y = \pm 0.50$ m), both ending at the same final height ($z = 0.50$ m). One of the stairs has three high steps, while the other has six lower steps. The goal of the robot is to reach a distant centered position $(x, y, z) = (3, 0, 0.5)$ m. The energy cost should be the same if the stairs were identical. We show the obtained footstep plan in Fig. 8. The figure shows that the planner opts for the lower-but-many-steps stairs. The reason for this result is that on steep stairs, steps become too costly for the distance traveled. Notice that the slope of the energetic cost E_{COM} in Fig. 3 is high in the direction of the step height. We will further analyze the

TABLE I
ESTIMATED ELECTRICAL ENERGY CONSUMPTION OF OUR PLANNER USING DIFFERENT OBJECTIVE FUNCTIONS

Scenario	E_{COM} (this paper)	Suboptimal E_{COM}	Travel time	Sum-of-torques	E_{ele} (ideal energy consumption)
Narrow ice $\mu = 0.12$	2110 J	+14%	+26%	−11%	−25%
Narrow ice $\mu = 0.06$	2427 J	+19%	+51%	−3%	−12%
Wide ice $\mu = 0.06$	3031 J	+10%	+92%	−13%	−18%
Stairs $\mu = 1$	4116 J	+9%	+40%	+0.5%	−13%
Slope $\mu = 1, \alpha = 25^\circ$	4908 J	+1%	+97%	(failed)	−5%

*Note: Reported energy is the estimated electrical energy consumption (6). Percentage values represent additional energy as a percentage of E_{COM} (i.e., $(E' - E_{\text{COM}})/E_{\text{COM}}$). "Suboptimal E_{COM}": refers to a plan that takes a suboptimal navigation option (i.e., around the ice instead of through, through instead of around, using the few-but-high-step stairs, walking straight on a 25° slope instead of in a curve) although still optimizing E_{COM} given that constraint.

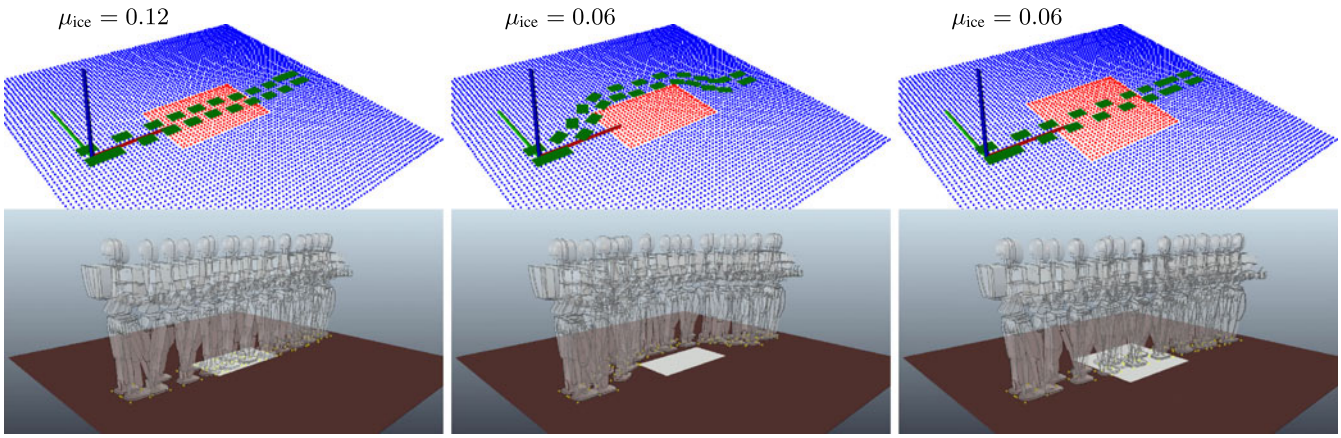

Fig. 6. Optimal plans obtained by our planner in the "ground and ice-patch" scenario. The top row shows the footstep plan and point cloud (red has friction μ_{ice}, blue $\mu_{\text{ground}} = 1$). (Left) Robot crosses a narrow ice patch ($\mu_{\text{ice}} = 0.12$). (Middle) Robot walks around the patch if its slipperiness is increased ($\mu_{\text{ice}} = 0.06$). (Right) Robot walks slowly through the same ice patch in case the ice is wider (energy spent avoiding it would be too high).

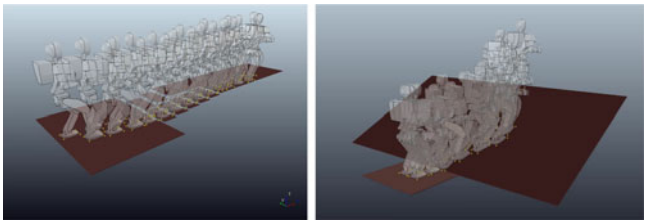

Fig. 7. Optimal plan obtained by our planner in the Stairs scenario (left) and Slope $\alpha = 25^\circ$ scenario (right). Shallower stairs and slopes have lower cost.

cost of slanted locomotion in Section VI-D. In terms of expected electrical energy (see Table I), our planner's path was 13% away from the true minimum of E_{ele}. The suboptimal choice of taking the few-but-high stairs would increase consumption by 9% and optimizing travel time would also increase consumption by 40%. Optimizing joint torques lead to basically the same performance as E_{COM} (0.5% more energy).

The final scenario was as follows. The robot has to climb a slope to a target that is straight ahead, 2.5 m away measured on a straight line connecting the start and target points. The slope has an angle of $\alpha \in \{10, 20, 25\}^\circ$. We show the planner results in Fig. 8 and the simulation in Fig. 7. The optimal path for the two shallowest slopes was in a straight line to the target, but for $\alpha = 25^\circ$ the optimal path was curved and at a slightly lower inclination. These results match observations in human mountain paths, as we will discuss in Section VI-D. In terms of expected electrical energy (see Table I), our planner's path for the 25° slope is only 5% away from the true minimum of E_{ele}. The suboptimal choice of taking a straight path to the target, instead of curved, would increase consumption by 1%. Optimizing travel time would increase consumption drastically, by 97%. Obtaining a path by optimizing joint torques was revealed to be unfeasible for our planner's time limit (which was 10 min), while an optimal plan was returned for E_{COM} in 10 s. By analyzing our model and planner data, our conclusion is that the sum-of-torques function has high variance due to noise in simulated joint torque measurements, and its optimization is prone to get stuck in local optima. The electrical energy minimizing planner also includes a joint torques term and, correspondingly, also took longer to solve the path to optimality (177 s) than when using COM work.

For all scenarios, our E_{COM}-optimal planner found a first suboptimal path within 1 s and the optimal path within 1 min. The computational speed improvement obtained by using precomputed energy costs for different step–friction combinations was of around one order of magnitude for both the initial and optimal paths. The ODE-simulated robot successfully walked without falling in all situations, even at high slipperiness and slope levels.

From the optimal-versus-suboptimal experiments, our results indicate that E_{COM} correlates well with E_{ele}. Still, it was less

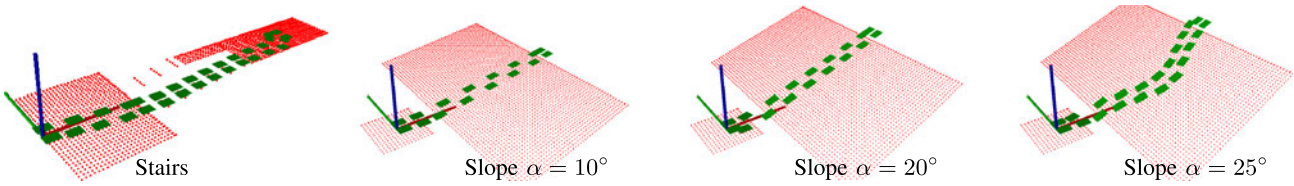

Fig. 8. Optimal plans obtained by our planner in the "Stairs" and "Slope" scenarios. On steep stairs and slopes, it is more energy optimal to walk a longer inclined distance but at a lower angle.

susceptible to local minima and long planning times than E_{ele} or torque minimization. These three quantities (E_{COM}, E_{ele}, and sum of torques) are all actually related to each other: Pearson correlation on data used for energy model training was $r = 0.78$ between joint torques and E_{ele}, $r = 0.54$ between joint torques and E_{COM}, $r = 0.58$ between E_{COM} and E_{ele}, and $r = 0.64$ between E_{COM} and joint mechanical work. Practically, for our setup, the human-inspired E_{COM} seems to be the best objective function choice as a compromise between energy consumption and computation time. Better optimization techniques could probably make direct optimization of E_{ele} more interesting, but in any case our proposed planner can be applied to both functions.

D. Comparison With Human Observations

The optimization objectives and variables proposed in this paper were inspired by human gait literature, as described in Section III. We now compare the results of our models and planner with the observations in human gait mentioned in that section.

1) Gradient of Mountain Paths [28], [29]: As we showed in model and planning results in Figs. 3, 7, and 8, high E_{COM} of slanted terrain leads to a preference of our planner for shallower slopes. In our example scenarios, the robot took low-step stairs and a curved 20° path on a steep 25° slope. Likewise in humans, mountain paths are predicted by oxygen consumption experiments on slopes [28], [29]. According to [29], humans prefer to climb steep mountains at a maximum inclination of approximately 14° and, in order to do that, they climb not straight to the mountain peak but in a curved pattern. Mountain path observations are also partly reproduced by assuming minimization of COM mechanical work [29], which is our objective function in this paper. In Fig. 9 we plot the chosen climbing angle versus the straight-line slope angle both for humans and our robot. The curve corresponding to humans was obtained by the data in [29]. The curve's shape is the same for humans and our robot: straight-line path until a certain angle, constant lower climbing angle after that. The angle at which this transition occurs is however different (approximately 14° for humans, 20° for the robot). We believe this to be due to differences in motor efficiency since WABIAN-2's weight, dimensions and joint positions are inspired by humans. We calculated the extra (constant) energy consumption of humans that would lead to the same plot as our robot's, and found it to be 0.5cal/kg/m. This curve is also shown in Fig. 9.

2) Horizontal Cost of Transport [33], [35]: The plots in Fig. 4 showed energy consumption per step. A known result from human biomechanics is, however, on the energetic cost

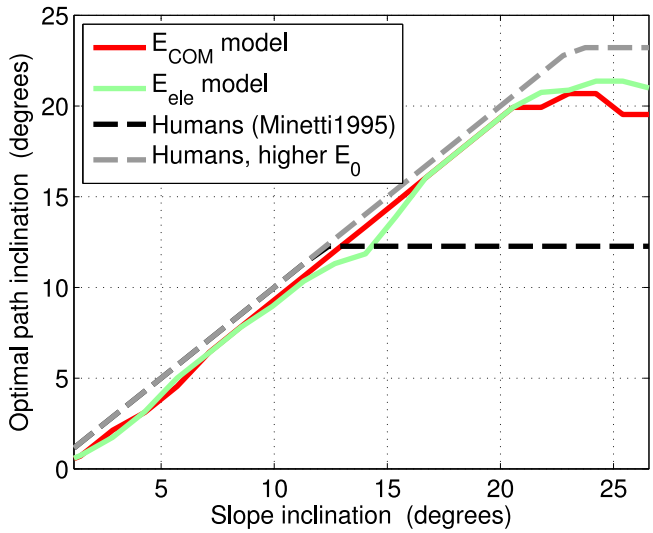

Fig. 9. Optimal path inclination angle α_{path} as a function of the slope angle α. If $\alpha_{\text{path}} < \alpha$, then the path is curved at a shallower inclination and a longer total distance.

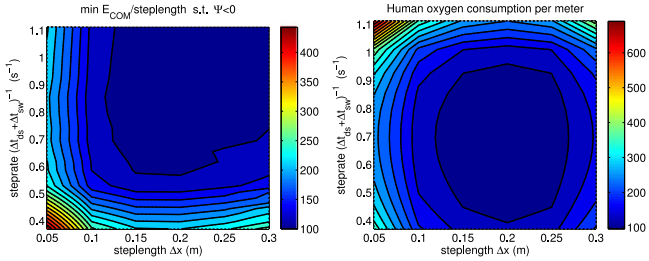

Fig. 10. (Left) Our robot's minimum E_{COM} per distance traveled. (Right) Oxygen consumption of a human with WABIAN-2's physical limits, given by the empirical formulas of human walking of [33]. Units are in percentage of the minimum.

per distance (i.e., cost of transport). The contours of human oxygen consumption per meter in steplength–steprate space actually resemble a hyperbola [33]. An empirical formula explaining this data was estimated by Zarrugh, Todd, and Ralston [33], which we used to compute the energy consumption of a human with WABIAN-2's physical limits (maximum step length 0.35 m, maximum step rate 1.20). Fig. 10 shows the humans' cost of transport prediction, as well as WABIAN-2's actual cost of transport (i.e. minimum E_{COM} per distance). The hyperbolic shape of the energy contours is similar to both humans and robot. The energy minimum seems to be slightly shifted towards a higher step rate in the robot's case, which we assume to be due to motor efficiency once again, although it could also be

related to a lower range of motion of the knees in our robot (up to 45 instead of 60 degrees). The similar shape is not surprising since it has also been reproduced by computer simulations of a simple bipedal walking model [35] using COM work optimization during toe-off.

3) Required Coefficient of Friction [20], [21], [25], [27]: Fig. 5, which shows the robot's RCOF model, also matches observations in human gait. The figure shows that the higher the Δt_{ds}, the lower the RCOF. In addition to that, the lower the step length, the lower the RCOF. According to [21], humans reduce RCOF (the shear-to-normal force ratio) when walking on slippery terrain, which in our planner we assume to be a walking constraint such that RCOF $< \mu$. The higher double-support observation means that to be able to walk on more slippery terrain (lower RCOF), the robot should opt for a conservative gait that is more static, with lower tangential speeds and accelerations. In addition, in humans a "cautious," more static, gait has been observed in humans walking on slippery terrain [20]–[22], as referred to in Section II-B. On the other hand, Llewellyn and Nevola [27] specifically observed an increase in double-support time when walking on slippery terrain. Regarding step length, the authors of [20], [21], and [25] also observed that this variable is lower when humans walk on slippery terrain. Reduction of step length is actually an anticipation strategy used just before stepping on slippery terrain [20], [21], [25]; just as in our robot's case, it is planned by assuming a constraint on RCOF [21]. While our planner uses a hard RCOF constraint, the decision was mainly motivated for practical and conservative reasons: a hard constraint lowers the risk of falling by theoretically avoiding slippage completely and thus not having to rely heavily on reactive slippage control. Humans, on the other hand, could possibly use RCOF or a related metric as a soft constraint, although we are not aware of any investigation on these lines.

VII. Conclusion and Discussion

In this paper, we have shown that optimal footstep planning for humanoid robots, by using simple principles and gait representations from human gait literature, leads to both human-like walking behavior and low electrical power consumption. Importantly, we showed through several simulation experiments that the planner we proposed here is well suited for challenging outdoor scenarios, since it accounts for ground friction and energy consumption.

We proposed a footstep planning algorithm with a human-inspired objective (COM work), constraint (RCOF) and variables (step length, width, height, double support time, swing time and knee flexion). We showed that our models and planner lead to a number of interesting observations such as: human-like RCOF, step length and double support time changes on slippery terrain, human-like curved walking on steep slopes after 20°, and hyperbolic contours of energy per distance in steplength-steprate plots. By estimating DC-motor electrical power consumption from simulation data, we also showed that planned paths had close to optimal electrical consumption, and that higher COM work leads to higher electrical energy. These observations and the simplicity of the model suggest COM work to be an effective objective function for planning of robot locomotion.

Some points in this paper may be important to discuss.

1) *Footstep planning with a learned model:* Our footstep planner relies on learned models of energy and slippage to plan optimal footstep sequences. These models depend on both the robot and whole-body controller used. Therefore, the models we obtained might differ from the ones obtained with different robots or using different controllers. The approach is still general and all that is required to apply our planner is to learn the E_{COM}, RCOF, and Ψ models in simulation with the desired robot and controller.
2) *Energy consumption:* We show that COM work is related to electrical energy consumption. However, at the cost of using a more complex model, further energy savings can be obtained by directly optimizing energy consumption. In addition, an interesting extension of our work would be to use the footstep planner's path as an initialization to a full-body trajectory optimization algorithm with the same objective.
3) *Coefficient of friction estimation:* The planner proposed here relies on the knowledge of the coefficient of friction between the robot's foot and the ground. While its estimation might be difficult in practice, we believe material classification from images and tabled COFs is a feasible approach to the problem. In addition, the planner can still be applied when uncertainty in the estimation is considered. For example, a margin can be added to the RCOF constraint depending on the expected uncertainty.
4) *Feasibility model:* The use of a feasibility model learned in the simulation was crucial in our experiments. One of the problems in footstep planning is to generate a plan for which whole-body motion is feasible. In practice, we found heuristic limits on stance distances to be insufficient due to unmodeled kinematics and dynamic unfeasibility. Learning feasibility as a function of step parameters alleviated this problem and sped planning up considerably, since more stances and steps were discarded early on.
5) *Planning footstep timing:* This paper importantly shows that planning time variables along with footstep placement is crucial when including ground friction in the problem. The RCOF for a slip to occur decreases with the decrease of step length and with the increase of double-support time, thus allowing the robot to walk on very slippery surfaces by adjusting these variables (as happens with humans [20], [21], [25], [27]). This also contrasts with the common practice in humanoid robotics to use constant step times.
6) *Search speed:* We compute parameters other than footstep placement from state transitions, which reduces the A* search space and increases search speed. Precomputing energetic cost for many combinations of footstep placement and μ also allowed for faster search than if (4) were to be solved explicitly for each state expansion. Instead, we solve it only for the final obtained path, reducing computation speed by one order of magnitude. In addition, in this paper, collision checking was not necessary due to the absence of obstacles in the tested scenarios. We expect current computational times to increase when adding a collision checking algorithm to the problem.

REFERENCES

[1] M. Brandão, K. Hashimoto, J. Santos-Victor, and A. Takanishi, "Gait planning for biped locomotion on slippery terrain," in *Proc. 14th IEEE-RAS Int. Conf. Humanoid Robots*, Nov. 2014, pp. 303–308.

[2] M. Brandão, K. Hashimoto, J. Santos-Victor, and A. Takanishi, "Optimizing energy consumption and preventing slips at the footstep planning level," in *Proc. 15th IEEE-RAS Int. Conf, Humanoid Robots*, Nov. 2015, pp. 1–7.

[3] W. Huang, J. Kim, and C. Atkeson, "Energy-based optimal step planning for humanoids," in *Proc. IEEE Int. Conf. Robot. Autom.*, May 2013, pp. 3124–3129.

[4] J. Kim, N. Pollard, and C. Atkeson, "Quadratic encoding of optimized humanoid walking," in *Proc. 13th IEEE-RAS Int. Conf. Humanoid Robots*, Oct. 2013, pp. 300–306.

[5] J. Chestnutt, M. Lau, G. Cheung, J. Kuffner, J. Hodgins, and T. Kanade, "Footstep planning for the Honda ASIMO humanoid," in *Proc. IEEE Int. Conf. Robot. Autom.*, Apr. 2005, pp. 629–634.

[6] J. Garimort and A. Hornung, "Humanoid navigation with dynamic footstep plans," in *Proc. IEEE Int. Conf. Robot. Autom.*, May 2011, pp. 3982–3987.

[7] A. Hornung, A. Dornbush, M. Likhachev, and M. Bennewitz, "Anytime search-based footstep planning with suboptimality bounds," in *Proc. 12th IEEE-RAS Int. Conf. Humanoid Robots*, Nov. 2012, pp. 674–679.

[8] K. Hauser, T. Bretl, J.-C. Latombe, K. Harada, and B. Wilcox, "Motion planning for legged robots on varied terrain," *Int. J. Robot. Res.*, vol. 27, nos. 11/12, pp. 1325–1349, 2008.

[9] H. Dai, A. Valenzuela, and R. Tedrake, "Whole-body motion planning with centroidal dynamics and full kinematics," in *Proc. 14th IEEE-RAS Int. Conf. Humanoid Robots*, Nov. 2014, pp. 295–302.

[10] R. Deits and R. Tedrake, "Footstep planning on uneven terrain with mixed-integer convex optimization," in *Proc. 14th IEEE-RAS Int. Conf. Humanoid Robots*, Nov. 2014, pp. 279–286.

[11] K. Hauser, T. Bretl, K. Harada, and J.-C. Latombe, "Using motion primitives in probabilistic sample-based planning for humanoid robots," in *Algorithmic Foundation of Robotics VII*. New York, NY, USA: Springer, 2008, pp. 507–522.

[12] N. Perrin, O. Stasse, L. Baudouin, F. Lamiraux, and E. Yoshida, "Fast humanoid robot collision-free footstep planning using swept volume approximations," *IEEE Trans. Robot.*, vol. 28, no. 2, pp. 427–439, Apr. 2012.

[13] S. Kajita, K. Kaneko, K. Harada, F. Kanehiro, K. Fujiwara, and H. Hirukawa, "Biped walking on a low friction floor," in *Proc. 2004 IEEE/RSJ Int. Conf. Intell. Robots Syst.*, vol. 4, Sep. 2004, pp. 3546–3552.

[14] J. H. Park and O. Kwon, "Reflex control of biped robot locomotion on a slippery surface," in *Proc. IEEE Int. Conf. Robot. Autom.*, vol. 4, 2001, pp. 4134–4139.

[15] M. Nikolic, B. Branislav, and M. Rakovic, "Walking on slippery surfaces: Generalized task-prioritization framework approach," in *Advances on Theory and Practice of Robots and Manipulators (ser. Mechanisms and Machine Science)*, vol. 22, M. Ceccarelli and V. A. Glazunov, Eds. New York, NY, USA: Springer, 2014, pp. 189–196.

[16] S. Feng, X. Xinjilefu, W. Huang, and C. Atkeson, "3D walking based on online optimization," in *Proc. 13th IEEE-RAS Int. Conf. Humanoid Robots*, Oct. 2013, pp. 21–27.

[17] S. Kajita *et al.*, "Biped walking pattern generation by using preview control of zero-moment point," in *Proc. IEEE Int. Conf. Robot. Autom.*, vol. 2, Sep. 2003, pp. 1620–1626.

[18] E. J. Gibson, G. Riccio, M. A. Schmuckler, T. A. Stoffregen, D. Rosenberg, and J. Taormina, "Detection of the traversability of surfaces by crawling and walking infants." *J. Exp. Psychol.: Hum. Perception Perform.*, vol. 13, no. 4, p. 533, 1987.

[19] K. E. Adolph, A. S. Joh, and M. A. Eppler, "Infants' perception of affordances of slopes under high-and low-friction conditions." *J. Exp. Psychol.: Hum. Perception Perform.*, vol. 36, no. 4, p. 797, 2010.

[20] G. Cappellini, Y. P. Ivanenko, N. Dominici, R. E. Poppele, and F. Lacquaniti, "Motor patterns during walking on a slippery walkway," *J. Neurophysiol.*, vol. 103, no. 2, pp. 746–760, 2010.

[21] R. Cham and M. S. Redfern, "Changes in gait when anticipating slippery floors," *Gait Posture*, vol. 15, no. 2, pp. 159–171, 2002.

[22] T. L. Heiden, D. J. Sanderson, J. T. Inglis, and G. P. Siegmund, "Adaptations to normal human gait on potentially slippery surfaces: The effects of awareness and prior slip experience," *Gait Posture*, vol. 24, no. 2, pp. 237–246, 2006.

[23] J. G. Buckley, K. J. Heasley, P. Twigg, and D. B. Elliott, "The effects of blurred vision on the mechanics of landing during stepping down by the elderly," *Gait Posture*, vol. 21, no. 1, pp. 65–71, 2005.

[24] H. B. Menz, S. R. Lord, R. S. George, and R. C. Fitzpatrick, "Walking stability and sensorimotor function in older people with diabetic peripheral neuropathy1," *Arch. Phys. Med. Rehabil.*, vol. 85, no. 2, pp. 245–252, 2004.

[25] J. C. Menant, J. R. Steele, H. B. Menz, B. J. Munro, and S. R. Lord, "Effects of walking surfaces and footwear on temporo-spatial gait parameters in young and older people," *Gait Posture*, vol. 29, no. 3, pp. 392–397, 2009.

[26] A. J. Chambers, S. Margerum, M. S. Redfern, and R. Cham, "Kinematics of the foot during slips," *Occup. Ergon.*, vol. 3, no. 4, pp. 225–234, 2002.

[27] M. G. A. Llewellyn and V. R. Nevola, "Strategies for walking on low-friction surfaces," in *Proc. 5th Int. Conf. Environ. Ergon.*, Maastricht, The Netherlands, 1992, pp. 156–157.

[28] R. M. Alexander, *Principles of Animal Locomotion*. Princeton, NJ, USA: Princeton Univ. Press, 2003.

[29] A. Minetti, "Optimum gradient of mountain paths," *J. Appl. Physiol.*, vol. 79, no. 5, pp. 1698–1703, 1995.

[30] D. R. Proffitt, M. Bhalla, R. Gossweiler, and J. Midgett, "Perceiving geographical slant," *Psychonomic Bull. Rev.*, vol. 2, no. 4, pp. 409–428, 1995.

[31] J. M. Wang, D. J. Fleet, and A. Hertzmann, "Optimizing walking controllers for uncertain inputs and environments," *ACM Trans. Graph.*, vol. 29, no. 4, pp. 73:1–73:8, Jul.2010.

[32] D. A. Winter, *Biomechanics and Motor Control of Human Gait: Normal, Elderly and Pathological*, 2nd ed. Waterloo, ON, Canada: Univ. Waterloo Press, 1991.

[33] M. Zarrugh, F. Todd, and H. Ralston, "Optimization of energy expenditure during level walking," *Eur. J. Appl. Physiol. Occup. Physiol.*, vol. 33, no. 4, pp. 293–306, 1974.

[34] A. Minetti and R. Alexander, "A theory of metabolic costs for bipedal gaits," *J. Theor. Biol.*, vol. 186, no. 4, pp. 467–476, 1997.

[35] A. D. Kuo, "A simple model of bipedal walking predicts the preferred speed–step length relationship," *J. Biomech. Eng.*, vol. 123, no. 3, pp. 264–269, 2001.

[36] B. R. Umberger and P. E. Martin, "Mechanical power and efficiency of level walking with different stride rates," *J. Exp. Biol.*, vol. 210, no. 18, pp. 3255–3265, 2007.

[37] K. Sasaki, R. R. Neptune, and S. A. Kautz, "The relationships between muscle, external, internal and joint mechanical work during normal walking," *J. Exp. Biol.*, vol. 212, no. 5, pp. 738–744, 2009.

[38] D. A. Winter, "A new definition of mechanical work done in human movement," *J. Appl. Physiol.*, vol. 46, no. 1, pp. 79–83, 1979.

[39] J. S. Matthis and B. R. Fajen, "Humans exploit the biomechanics of bipedal gait during visually guided walking over complex terrain," in *Proc. R. Soc. London B, Biol. Sci.*, vol. 280, no. 1762, p. 2013, 2013.

[40] H. B. Menz, S. R. Lord, and R. C. Fitzpatrick, "Acceleration patterns of the head and pelvis when walking on level and irregular surfaces," *Gait Posture*, vol. 18, no. 1, pp. 35–46, 2003.

[41] D. Fong, Y. Hong, and J. X. Li, "Lower-extremity gait kinematics on slippery surfaces in construction worksites," *Med. Sci. Sports Exercise*, vol. 37, no. 3, pp. 447–454, 2005.

[42] K. Mombaur, A. Truong, and J.-P. Laumond, "From human to humanoid locomotionan inverse optimal control approach," *Auton. Robots*, vol. 28, no. 3, pp. 369–383, 2010.

[43] S. Collins and A. Ruina, "A bipedal walking robot with efficient and human-like gait," in *Proc. IEEE Int. Conf. Robot. Autom.*, Apr. 2005, pp. 1983–1988.

[44] K. Hashimoto, H. Kondo, H.-O. Lim, and A. Takanishi, "Online walking pattern generation using FFT for humanoid robots," in *Motion and Operation Planning of Robotic Systems: Background and Practical Approaches*. New York, NY, USA: Springer, 2015, pp. 417–438.

[45] B. Damas and J. Santos-Victor, "Online learning of single-and multivalued functions with an infinite mixture of linear experts," *Neural Comput.*, vol. 25, no. 11, pp. 3044–3091, 2013.

[46] M. Likhachev, G. J. Gordon, and S. Thrun, "Ara*: Anytime a* with provable bounds on sub-optimality," in *Proc. Conf. Adv. Neural Inf. Process. Syst.*, 2003, pp. 767–774.

[47] R. B. Rusu and S. Cousins, "3D is here: Point Cloud Library (PCL)," presented at the *IEEE Int. Conf. Robot. Autom.*, Shanghai, China, May 9–13, 2011.

[48] M. Likhachev, *Search-based planning library*. 2010. [Online]. Available: http://www.ros.org/wiki/sbpl

[49] D. R. Jones, C. D. Perttunen, and B. E. Stuckman, "Lipschitzian optimization without the Lipschitz constant," *J. Optim. Theory Appl.*, vol. 79, no. 1, pp. 157–181, 1993. [Online]. Available: http://dx.doi.org/10.1007/BF00941892

[50] D. Kraft, "Algorithm 733: Tomp–Fortran modules for optimal control calculations," *ACM Trans. Math. Softw.*, vol. 20, no. 3, pp. 262–281, Sep. 1994.
[51] S. G. Johnson, *The NLopt nonlinear-optimization package*. (2014). [Online]. Available: http://ab-initio.mit.edu/nlopt
[52] J. Perry, *Gait Analysis: Normal and Pathological Function*. Thorofare, NJ, USA: Slack, 1992.
[53] M. Freese, S. Singh, F. Ozaki, and N. Matsuhira, " Virtual robot experimentation platform v-rep: A versatile 3d robot simulator," in *Simulation, Modeling, and Programming for Autonomous Robots* (ser. Lecture Notes in Computer Science), vol. 6472. New York, NY, USA: Springer, 2010, pp. 51–62.
[54] *E C Corporation, DC Motors, Speed Controls, Servo Systems*. New York, NY, USA: Pergamon, 1977.

Martim Brandão (M'11) received the M.Sc. degree in electrical and computer engineering from Instituto Superior Técnico, IST, Lisbon, Portugal, in 2010. He is currently working toward the Ph.D. degree with Waseda University, Tokyo, Japan.

He was a Research Assistant with the Computer and Robot Vision Laboratory, IST, in 2011 and a Research Student with Takanishi Laboratory, Waseda University, until 2013. His research interests include human-inspired robot motion planning and vision-related topics for robot locomotion.

Kenji Hashimoto (M'05) received the B.E. and M.E. degrees in mechanical engineering in 2004 and 2006, respectively, and the Ph.D. degree in integrative bioscience and biomedical engineering in 2009, all from Waseda University, Tokyo, Japan.

He is an Assistant Professor the Waseda Institute for Advanced Study, Waseda University. His research interests include walking systems, biped robots, and humanoid robots.

José Santos-Victor (SM'85) received the Ph.D. degree in electrical and computer engineering from the Computer and Robot Vision Laboratory, Instituto Superior Técnico (IST), Lisbon, Portugal, in 1995.

He is a Full Professor with IST and a Researcher with the Institute for Systems and Robotics, Universidade de Lisboa, Lisbon, where he founded the Computer and Robot Vision Laboratory. His research interests include computer and robot vision, particularly visual perception and the control of action, and biologically inspired vision and robotics.

Atsuo Takanishi (M'95) received the B.S.E., M.S.E., and Ph.D. degrees in mechanical engineering from Waseda University, Tokyo, Japan, in 1980, 1982, and 1988, respectively.

He is a Professor with the Department of Modern Mechanical Engineering, Waseda University, where he is also the Director of the Humanoid Robotics Institute. His research interests include humanoid robots and its applications in medicine and well-being.